Perturbation of Cytochrome *c* Maturation Reveals Adaptability of the Respiratory Chain in *Mycobacterium tuberculosis*

Jennifer L. Small,[a] Sae Woong Park,[a] Bavesh D. Kana,[b] Thomas R. Ioerger,[c] James C. Sacchettini,[c] Sabine Ehrt[a]

Department of Microbiology and Immunology, Weill Cornell Medical College, New York, New York, USA[a]; DST/NRF Centre of Excellence for Biomedical TB Research, Faculty of Health Sciences, University of the Witwatersrand and the National Health Laboratory Service, Johannesburg, South Africa[b]; Department of Biochemistry and Biophysics, Texas A&M University, College Station, Texas, USA[c]

ABSTRACT ***Mycobacterium tuberculosis*** **depends on aerobic respiration for growth and utilizes an aa_3-type cytochrome *c* oxidase for terminal electron transfer. Cytochrome *c* maturation in bacteria requires covalent attachment of heme to apocytochrome *c*, which occurs outside the cytoplasmic membrane. We demonstrate that in *M. tuberculosis* the thioredoxin-like protein Rv3673c, which we named CcsX, is required for heme insertion in cytochrome *c*. Inactivation of CcsX resulted in loss of *c*-type heme absorbance, impaired growth and virulence of *M. tuberculosis*, and induced cytochrome *bd* oxidase. This suggests that the bioenergetically less efficient *bd* oxidase can compensate for deficient cytochrome *c* oxidase activity, highlighting the flexibility of the *M. tuberculosis* respiratory chain. A spontaneous mutation in the active site of vitamin K epoxide reductase (VKOR) suppressed phenotypes of the CcsX mutant and abrogated the activity of the disulfide bond-dependent alkaline phosphatase, which shows that VKOR is the major disulfide bond catalyzing protein in the periplasm of *M. tuberculosis*.**

IMPORTANCE ***Mycobacterium tuberculosis*** **requires oxygen for growth; however, the biogenesis of respiratory chain components in mycobacteria has not been explored. Here, we identified a periplasmic thioredoxin, CcsX, necessary for heme insertion into cytochrome *c*. We investigated the consequences of disrupting cytochrome *c* maturation (CCM) for growth and survival of *M. tuberculosis in vitro* and for its pathogenesis. Appearance of a second-site suppressor mutation in the periplasmic disulfide bond catalyzing protein VKOR indicates the strong selective pressure for a functional cytochrome *c* oxidase. The observation that *M. tuberculosis* is able to partially compensate for defective CCM by upregulation of the cytochrome *bd* oxidase exposes a functional role of this alternative terminal oxidase under normal aerobic conditions and during pathogenesis. This suggests that targeting both oxidases simultaneously might be required to effectively disrupt respiration in *M. tuberculosis*.**

Received 26 June 2013 **Accepted** 23 August 2013 **Published** 17 September 2013

Citation Small JL, Park SW, Kana BD, Ioerger TR, Sacchettini JC, Ehrt S. 2013. Perturbation of cytochrome *c* maturation reveals adaptability of the respiratory chain in *Mycobacterium tuberculosis*. mBio 4(5):e00475-13. doi:10.1128/mBio.00475-13.

Editor Roberto Kolter, Harvard Medical School

Address correspondence to Sabine Ehrt, sae2004@med.cornell.edu.

Mycobacterium tuberculosis has evolved to survive for decades within host granulomas. An infected host often develops different types of granulomas, including caseating, fibrotic, and cavitating lesions, each providing a different environment (1, 2). Even bacteria within the same lesion may experience different microenvironments depending on their location within the granuloma (3), and they can exist as multiple subpopulations (4). The availability of oxygen and nutrients can also differ vastly between various *in vivo* niches. It has been shown that *M. tuberculosis*, while residing in cavities, experiences the same oxygen tension as in the bronchi in the lung (5). However, *M. tuberculosis* further away from the cavity surface or localized in noncavitating lesions is exposed to microaerobic or anaerobic conditions (6). Thus, throughout the course of infection, even within the same lesion, *M. tuberculosis* must adapt its metabolism to survive and persist. The ability of *M. tuberculosis* to adapt to multiple environments can in part be attributed to the modulatory nature of its respiratory chain (7, 8). Electrons flow from NADH dehydrogenase and succinate dehydrogenase complexes into the menaquinone-menaquinol pool, terminating at either the cytochrome bc_1-aa_3 oxidoreductase supercomplex or the *bd*-type menaquinol oxidase (9–12). Both oxidases use O_2 as the terminal electron acceptor. The cytochrome bc_1-aa_3 oxidoreductase (CcO) supercomplex consists of a bc_1 di-heme *c*-type cytochrome reductase, encoded by *qcrCAB*, that transfers electrons to the terminal aa_3-type Cu-heme oxidase, encoded by *ctaB*, *ctaC*, *ctaD*, *ctaE*, and *ctaF* (8). Cytochromes of the *c* type are characterized by covalently bound heme, which is attached via two thioether bonds to the two cysteine residues in the heme binding motif Cys-Xxx-Xxx-Cys-His (13, 14). This cytochrome *c* maturation (CCM) occurs on the outside the cytoplasmic membrane (15). *M. tuberculosis* is predicted to use a type II CCM system, consisting of four proteins, that is best characterized in *Bacillus subtilis* (ResA, ResB, ResC, CcdA) and *Bordetella pertussis* (CcsA, CcsB, CcsX, DipZ) (16–19) (see Fig. S1 in the supplemental material). The integral membrane proteins ResB/CcsA bind heme in the cytoplasm and export it to the extracellular domains of ResC/CcsB, priming it for covalent attachment to apocytochrome *c*. Thiol reduction is catalyzed by CcdA/DipZ and the membrane-anchored thioredoxin-like protein, ResA/CcsX, which reduces the disulfide bond of the Cys-Xxx-

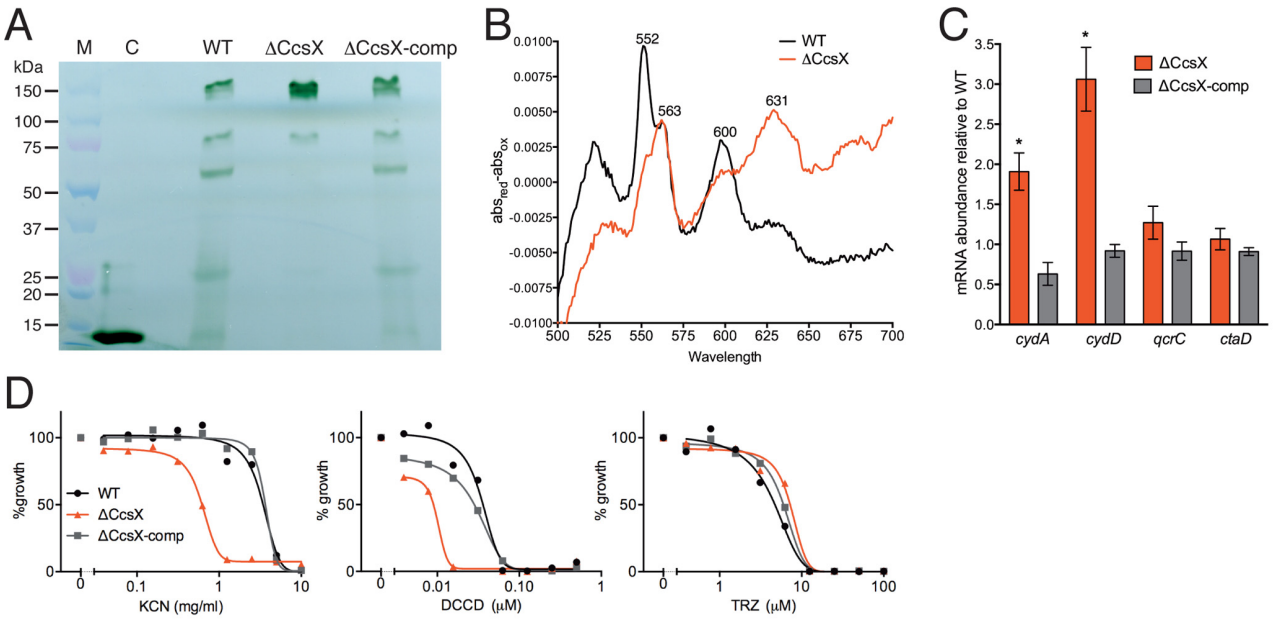

FIG 1 CcsX is important for cytochrome *c* maturation. (A) SDS-PAGE and heme staining of membranes from WT *M. tuberculosis* and the ΔCcsX and ΔCcsX-comp mutants. Horse heart cytochrome *c* (C) served as the positive control. (B) Sodium dithionite-reduced minus potassium ferricyanide-oxidized difference spectra of WT (black line) and ΔCcsX (red line) membranes. Data are means from two independent experiments. (C) Relative mRNA amounts of respiratory genes in ΔCcsX and ΔCcsX-comp mutants. mRNAs were quantified by quantitative real-time PCR and normalized to *sigA* and are expressed as abundance relative to mRNA levels in the WT. Error bars represent standard deviations (SD) from three biological replicates. Student's *t* test *P* values are indicated (*, $P < 0.05$). (D) Minimal inhibitory concentrations of respiratory chain inhibitors. Log-transformed drug concentrations were plotted against growth normalized to untreated cultures and fit with a nonlinear regression curve.

Xxx-Cys-His motif of apocytochrome *c* (18–21). In this study, we identified the ResA/CcsX homolog in *M. tuberculosis*, encoded by *rv3673c*, and investigated the consequences of disrupting cytochrome *c* biogenesis. We provide evidence that the bioenergetically less efficient cytochrome *bd* oxidase substitutes for impaired CcO activity and that loss of CcsX can be compensated for by a mutation in the disulfide bond-forming protein vitamin K epoxide reductase (VKOR).

RESULTS AND DISCUSSION

Identification of a membrane-bound, periplasmic thioredoxin. We sought to identify the gene encoding *M. tuberculosis*'s ResA/CcsX and searched for genes encoding proteins predicted to contain a thioredoxin fold and a single transmembrane helix or to be localized to the membrane, using the Tuberculist database (22) and the transmembrane prediction server, TMHMM version 2.0 (23). Of the proteins that matched our criteria, Rv0526 and Rv3673c were the most likely candidates, with 24% and 33% sequence identity to *B. subtilis* ResA, respectively. Rv3673c is predicted to contain a single transmembrane helix, and Rv0526 is predicted to be a secreted lipoprotein. We focused on Rv3673c because of its membrane-anchoring transmembrane helix and sequence similarity to ResA even though *rv0526* is located in the genomic region that contains the other predicted components of the CCM system. Based on the results of the work presented here, Rv3673 was named CcsX.

To experimentally confirm that the catalytic domain of CcsX is located in the periplasm, we created fusions with alkaline phosphatase (PhoA) at residues leucine 41, serine 47, and proline 65 and expressed them in *Mycobacterium smegmatis* (see Fig. S2 in the supplemental material). PhoA is active only when located in the oxidizing extracytoplasmic environment and has been used to determine the topology of membrane proteins (24), including those in mycobacteria (17, 25). All CcsX-PhoA fusions demonstrated alkaline phosphatase activity (see Fig. S2B in the supplemental material). A plasmid containing PhoA lacking a signal sequence served as a negative control, and a plasmid expressing PhoA fused to the signal sequence of the secreted antigen 85B served as our positive control (25). Immunoblot analysis of *M. tuberculosis* expressing Flag-tagged CcsX confirmed its association with the cell membrane/wall fraction (see Fig. S2C). Taken together, these data suggest that CcsX is a membrane-associated protein with an extracellular thioredoxin domain.

CcsX is required for heme insertion in cytochrome *c*, and cytochrome *bd* oxidase can compensate for loss of CcsX. We created an *M. tuberculosis* mutant strain, the ΔCcsX mutant, in the background of H37Rv, in which the entire *ccsX* gene was replaced with a hygromycin cassette. Deletion of *ccsX* was confirmed by Southern blotting (see Fig. S3 in the supplemental material). To determine the impact of loss of CcsX on CCM, we stained for proteins with covalently bound heme in membrane fractions of *M. tuberculosis* H37Rv wild type (WT), the ΔCcsX mutant, and the CcsX-comp complemented mutant. Heme staining of WT membranes revealed five bands at >150 kDa, ~80 kDa, ~60 kDa, ~25 kDa, and ~15 kDa (Fig. 1A), and we attempted to identify the proteins containing covalently bound heme. Liquid chromatography-tandem mass spectrometry (LC-MS/MS) revealed multiple proteins in each band, at least one of which had a predicted heme-binding motif. Using the LC-MS/MS data, heme-binding motif predictions, and molecular masses, we assigned a

heme-bound protein to each band. The band at ~80 kDa corresponds to the catalase-peroxidase KatG (26); the band at~60 kDa corresponds to SirA, a sulfite reductase with a covalently bound siroheme moiety (27); and the band at ~25 kDa stems from QcrC, the cytochrome *c* subunit of the bc_1 cytochrome *c* reductase complex (8). Attempts to identify the ~15-kDa protein were unsuccessful, and the 150-kDa band appeared to be an aggregate containing more than one of the heme-containing proteins found in the lower-molecular-mass bands. Heme staining of membranes from the ΔCcsX mutant did not reveal bands for SirA or the ~15-kDa protein, and the band corresponding to QcrC was drastically reduced in intensity (Fig. 1A). This strongly suggested that CcsX is important for cytochrome *c* assembly. Heme binding to KatG was unaffected by the lack of CcsX, which is not surprising, because KatG is cytosolic and should thus not depend on the extracytoplasmic thioredoxin CcsX for heme attachment. More surprising was the heme deficiency in SirA, formerly known as NirA, a sulfite reductase with covalently bound siroheme (27, 28). SirA is a predicted cytosolic protein and thus unlikely to rely on the extracytoplasmic CcsX for heme insertion. Siroheme can, however, be hijacked and processed into heme in some bacteria and archaea (29). The defective heme incorporation into QcrC may have resulted in excessive heme export and depletion of intracellular heme stores, which in turn caused conversion of siroheme to heme, thereby depleting siroheme in SirA. Alternatively, SirA might be an extracytoplasmic protein and directly rely on CcsX for siroheme acquisition, as proteomics identified SirA in the membrane/lipid fractions of *M. tuberculosis* (30, 31).

To confirm the loss of *c*-type heme incorporation into QcrC, reduced minus oxidized difference spectroscopy was used to analyze the cytochrome content of the aerobically grown WT and ΔCcsX strains. In WT membranes, major absorbance peaks were observed at 552, 563, and 600 nm, characteristic of *c*-, *b*-, and *a*-type cytochromes, respectively (9, 32) (Fig. 1B). In membranes from the ΔCcsX mutant, the major peak at 552 nm was no longer visible, indicating a lack of *c*-type heme. The peak at 563 nm was unchanged; however, a prominent peak was visible at 631 nm, which we did not observe in WT membranes. This peak is characteristic of a *d*-type heme and has been demonstrated to indicate the presence of the *bd* oxidase in *M. smegmatis* following exposure to microaerobic conditions ($O_2 < 1\%$) but was undetectable when the bacteria were grown aerobically (9). The *bd* terminal oxidase is also induced in *M. smegmatis* lacking the cytochrome bc_1 oxidase (12) and in *M. tuberculosis* treated with the cytochrome *c*-specific inhibitors cyanide and azide or agents affecting CCM, such as $ZnSO_4$ and dithiothreitol (DTT) (33). Consistent with the hypothesis that *bd* oxidase is upregulated in the ΔCcsX mutant to compensate for the perturbation in CCM, mRNA levels of genes of the *bd* oxidase encoding the *cyd* operon (*cydABDC*) were 2- to 3-fold higher in the mutant than in the WT, while expression levels of *qcrC* and *ctaD* were unchanged in the ΔCcsX mutant (Fig. 1C). Furthermore, the ΔCcsX mutant was hypersusceptible to cyanide and to the proton-translocating F_oF_1–ATP synthase inhibitor *N*,*N*′-dicyclohexylcarbodiimide (DCCD), suggesting impaired cytochrome *c* oxidase activity and reduced respiratory energy generation (Fig. 1D). In contrast, the minimal inhibitory concentration of thioridazine (TRZ), a phenothiazine derivative thought to inhibit the type II NADH dehydrogenase (11, 33, 34), was not different from that of the WT and the ΔCcsX-comp mutant, suggesting that type II NADH dehydrogenase activity is not decreased in the mutant.

Together, these data demonstrate that (i) CcsX is important for CCM in *M. tuberculosis*, (ii) Rv0526 is not functionally redundant with CcsX, and (iii) deletion of CcsX is accompanied by increased expression of *bd* oxidase, suggesting that defective CCM resulted in reduced electron flow through the bc_1-aa_3 oxidase, which can at least partially be compensated for by increased *bd* oxidase activity.

Deficient CCM is associated with increased resistance to H_2O_2. Consistent with transposon mutagenesis studies, which predicted *ccsX* to be required for optimal growth (35, 36), the ΔCcsX mutant grew slower than the WT on agar plates and in liquid medium (Fig. 2A and B). Introducing a copy of *ccsX* back onto the mutant chromosome complemented these phenotypes. Deletion of ResA/CcsX homologs caused increased resistance to H_2O_2 treatment in *Agrobacterium tumefaciens* (37) but hypersusceptibility to H_2O_2 in *Neisseria gonorrhoeae* (38). Consistent with the phenotype in *A. tumefaciens*, the ΔCcsX mutant was hyperresistant to H_2O_2 (Fig. 2C), and H_2O_2 hyperresistance was returned to WT levels in the complemented mutant, confirming that this phenotype was due to the loss of CcsX. This response was specific to H_2O_2 stress. Exposure to superoxide-generating plumbagin, acidified sodium nitrite resulting in the generation of reactive nitrogen species, and acidification (pH 4.5) did not affect the mutant differently than the WT (see Fig. S4 in the supplemental material). To explore the mechanism responsible for H_2O_2 hyperresistance, we measured expression of genes important for antioxidant defense in *M. tuberculosis* (39–42). There was no difference in *katG* mRNA or protein abundance between the ΔCcsX mutant and the WT (Fig. 2D and E), similar to the finding that H_2O_2 hyperresistance of the TlpA (CcsX homolog) mutant in *A. tumefaciens* was catalase independent (37). mRNA levels of the thioredoxin genes, *trxB1*, *thiX*, and the thioredoxin reductase-encoding *trxB2*, were also similar in all strains. In contrast, mRNA levels of alkyl hydroperoxide reductase (AhpC) were 2.5-fold increased in the ΔCcsX mutant and returned to WT levels in the complemented strain (Fig. 2D). Consistent with the increased mRNA levels, protein amounts of AhpC and AhpD, a thioredoxin-like adaptor protein (43), were also increased in the ΔCcsX mutant (Fig. 2E). AhpC and AhpD are subunits of *M. tuberculosis*'s peroxidase and peroxynitrite reductase complex and have been implicated in oxidative and nitrosative stress responses (39, 42, 43). However, deletion of *ahpC* in *M. tuberculosis* resulted in hypersusceptibility to cumene hydroperoxide but not H_2O_2 (44). The increased resistance to H_2O_2 of the ΔCcsX mutant may also be a consequence of overexpression of the cytochrome *bd* oxidase, as *E. coli cyd* mutants are hypersusceptible to H_2O_2 stress (45, 46). The cytochrome *bd* oxidase retains a high affinity for oxygen (47), and increased expression would result in efficient scavenging of oxygen radicals produced from the breakdown of H_2O_2, leading to increased resistance. Consistent with this is the observation that cytochrome *bd* oxidase plays a respiratory protective role for nitrogen-fixing enzymes which are sensitive to oxidative damage (48). It is noteworthy that unlike other terminal cytochrome oxidases, the cytochrome *bd* oxidase does not generate superoxide radicals during catalytic reduction of oxygen, which serves as a barrier for the formation of excessive endogenous oxidative species (49).

The role of CcsX in pathogenesis. Gene expression analysis revealed that genes encoding subunits of the cytochrome *c* oxidase

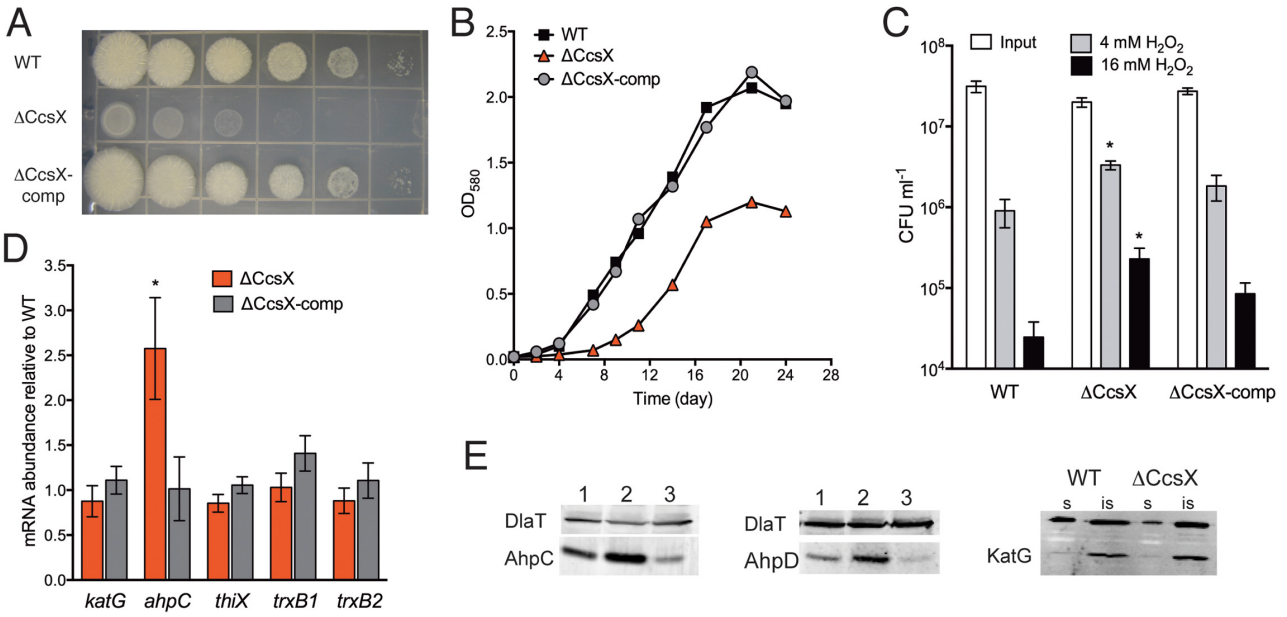

FIG 2 Deletion of CcsX results in impaired growth and increased resistance to H_2O_2. Growth of WT, ΔCcsX, and ΔCcsX-comp strains on agar plates (A) and in Sauton's liquid medium (B). (C) Survival of *M. tuberculosis* strains after exposure to hydrogen peroxide. Bacteria were plated and CFU were determined after exposure to 4 and 16 mM H_2O_2 for 4 h. Data are means ± SD of triplicate cultures and representative of two independent experiments (*, $P < 0.05$, compared to the WT and compared to the complemented strain). (D) Relative mRNA amounts of potential antioxidant genes in the ΔCcsX and ΔCcsX-comp mutants. mRNAs were quantified by quantitative real-time PCR and normalized to *sigA* and are expressed as abundance relative to mRNA levels in the WT. Error bars represent SD from three biological replicates. Student's *t* test *P* values are indicated (*, $P < 0.05$). (E) Immunoblot analysis of proteins extracts from the WT (lane 1), ΔCcsX (lane 2), and ΔCcsX-comp (lane 3) strains using antisera against AhpC, AhpD, KatG, and DlaT (loading control). Soluble (s) and insoluble (is) protein fractions were run for the KatG immunoblot.

and *bd* oxidase were differentially expressed at different phases of mouse infection (50). This suggested that cytochrome *c* oxidase is most important for *M. tuberculosis*'s ability to replicate during the acute phase, while the less-energy-efficient *bd* oxidase is preferentially required during transition from acute to chronic infection. The ΔCcsX mutant reached 100-fold-lower CFU than the WT in mouse lungs at day 21 following low-dose aerosol infections, after which it maintained a constant titer (Fig. 3A). A similar trend was observed in spleens, to which the ΔCcsX mutant disseminated more slowly than the WT and never reached the same bacterial load (Fig. 3A, right). Growth in lungs and spleens was restored to WT levels in the complemented mutant (Fig. 3B). Thus, perturbed CCM affected replication of *M. tuberculosis in vivo* but had no impact on persistence during chronic mouse infection. These data suggest that *bd* oxidase can sufficiently substitute for impaired cytochrome *c* oxidase activity during the chronic phase of the infection when the bacilli are only slowly or not replicating but are exposed to the host-adaptive immune response. In addition to fulfilling a respiratory role in the electron transport chain, cytochrome *bd* oxidase may protect tubercle bacilli against reactive oxygen species generated through the adaptive immune response. In contrast, normal replication early in infection depends on intact CCM and cytochrome *c* oxidase activity.

A VKOR mutation compensates for loss of CcsX. During the course of these experiments, especially after multiple passages, the ΔCcsX phenotypes became less robust. When plating the mutant

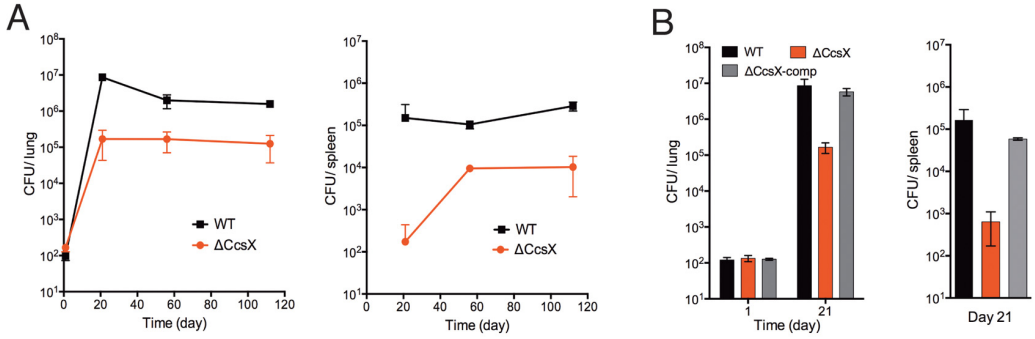

FIG 3 The ΔCcsX mutant is attenuated in the mouse model of tuberculosis. (A) Growth and survival in mouse lungs (left) and spleens (right) of the WT and ΔCcsX strains. Data are from 4 mice per strain and time point and representative of 2 independent experiments. (B) The ΔCcsX-comp strain grows like the WT in mouse lungs and spleens. Data are from 4 mice per strain and time point.

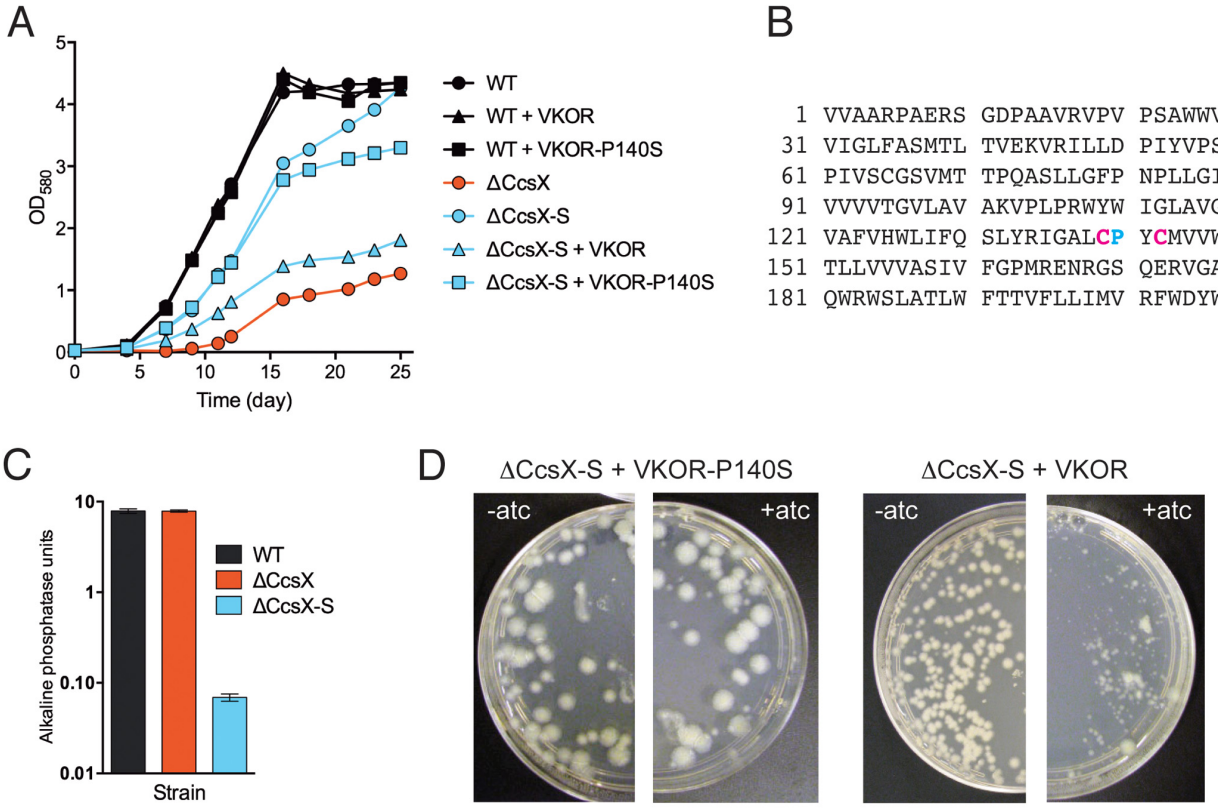

FIG 4 VKOR-P140S can suppress the defects caused by lack of CcsX. (A) Growth of *M. tuberculosis* strains in 7H9 medium containing 200 ng/ml atc. Expression of VKOR and VKOR-P140S was from an atc-inducible promoter on an episomal plasmid (66). (B) Amino acid sequence of VKOR. The cysteine residues in the active site are depicted in pink, and the proline residue, which is mutated to serine in the suppressor strain, is depicted in blue. (C) Alkaline phosphatase activity in *M. tuberculosis* strains transformed with a plasmid that constitutively expresses a fusion of antigen 85B-PhoA. (D) Growth of the ΔCcsX-S mutant transformed with VKOR-P140S and with wild-type VKPOR on agar plates with and without atc. Expression of VKOR and VKOR-P140S was from an atc-inducible promoter on an episomal plasmid (66).

on 7H10 agar, we noticed a heterogeneous population of colonies, with some significantly larger than others (see Fig. S5A in the supplemental material). Both small and big colonies lacked the *ccsX* gene, suggesting that the large colonies represented a suppressor mutant (see Fig. S5B and C in the supplemental material). This putative suppressor strain, the ΔCcsX-S mutant, also grew significantly faster than the ΔCcsX mutant in liquid medium (Fig. 4A) and was more susceptible to H_2O_2 than the ΔCcsX mutant (see Fig. S5D). Whole-genome sequencing revealed a point mutation in *rv2968c/vkor*, resulting in an amino acid change in vitamin K epoxide reductase (VKOR). *M. tuberculosis*'s VKOR is functionally similar to DsbB in *E. coli* (51, 52), which together with DsbA catalyzes disulfide bond formation in the periplasm (53). The ΔCcsX-S mutation caused the proline residue at position 140 to be replaced with a serine (Fig. 4B). This proline lies in the Cys-Xxx-Xxx-Cys thioredoxin active site and is conserved in most thioredoxin family members (54, 55). TMHMM predicts that this sequence in VKOR is located in the periplasmic space consistent with its function. To determine whether the substitution of proline with serine affected the function of VKOR, we expressed the antigen 85B secretion signal-PhoA fusion protein, whose activity depends on intramolecular disulfide bond formation (56), in the WT, the ΔCcsX mutant, and the ΔCcsX-S mutant and measured alkaline phosphatase activity. PhoA activity was drastically reduced in the ΔCcsX-S mutant compared to in the other strains, suggesting that the point mutation in VKOR-P140S impaired disulfide bond formation in the periplasm of the ΔCcsX-S mutant (Fig. 4C). Finally we complemented the ΔCcsX-S mutant with intact VKOR to prove that the suppressor phenotype was caused by the mutated VKOR. Expression of the native, intact *vkor* gene from a tetracycline repressor-controlled promoter in the ΔCcsX-S mutant resulted in small colonies, while expression of the mutated gene did not affect growth of the ΔCcsX-S mutant (Fig. 4D). Even in the absence of the inducer anhydrotetracycline (atc), the ΔCcsX-S mutant transformed with WT VKOR formed smaller colonies than when transformed with VKOR-P140S, likely because of leaky expression. The addition of atc exacerbated this phenotype. Similarly, growth of the ΔCcsX-S mutant expressing VKOR in atc-containing liquid medium was significantly reduced compared to that of the untransformed control and mimicked the slow growth of the ΔCcsX mutant (Fig. 4A). In contrast, the ΔCcsX-S mutant transformed with VKOR-P140S replicated like the untransformed ΔCcsX-S mutant, and the growth of the WT was not affected by either VKOR or VKOR-P140S. Together, these data demonstrate that the point mutation in VKOR caused the suppressor phenotype of the ΔCcsX-S mutant. Mutations in DsbA and DsbB in *Rhodobacter capsulatus* (57) and *B. subtilis* (58) have been demonstrated to compensate for the loss of CcdA and restore

cytochrome *c* biogenesis. CcdA and its redox partner ResA/CcsX are required for the periplasmic reduction of the disulfide bond in apocytochrome *c*, allowing heme attachment (19, 59). The redox pair DsbA and DsbB forms the disulfide; thus, mutation in either of these proteins or the addition of a reducing agent to the medium abrogates the need for CcdA and ResA/CcsX. Similarly, mutation of VKOR suppressed the defect caused by lack of CcsX. Together, these data not only establish that CcsX is part of *M. tuberculosis*'s CCM system but also support the hypothesis that VKOR is the major disulfide bond catalyzing protein in *M. tuberculosis*'s periplasm.

MATERIALS AND METHODS

Strains, media, and molecular biology techniques. *M. tuberculosis* (H37Rv) strains were grown in Middlebrook 7H9 or Sauton's medium as described (60). Cultures were grown aerated in roller bottles rotating at 1 rpm or in stationary tissue culture flasks in small volumes (10 ml) and agitated regularly to ensure aeration. Bacteria were also grown on Middlebrook 7H10 or 7H11 agar plates containing 10% oleic acid-albumin-dextrose-catalase (OADC) supplement (Becton Dickinson) and 0.5% glycerol. Hygromycin B (50 μg/ml), kanamycin (20 μg/ml), and streptomycin (20 μg/ml) were included when selection was required. The ΔCcsX mutant was constructed using a suicide plasmid (61). Gateway cloning technology (Invitrogen) was used for clonings (60). For complementation, *ccsX* was cloned downstream of the hsp60 promoter into a plasmid that integrates into the chromosomal *attB* site and electroporated into the ΔCcsX mutant. Alkaline phosphatase fusions were created and analyzed as described (25, 62). RNA isolation and analysis by quantitative real-time PCR was performed as described (60).

Heme staining and cytochrome spectra. *M. tuberculosis* lysates were prepared from mid-log-phase cultures, and membranes were isolated as described (63). Membranes for heme staining were resuspended in ammonium bicarbonate (NH_4HCO_3; Fisher) by sonication until dissolved. A total of 80 μg of membrane fraction was separated on a 4 to 15% Tris-HCl gradient gel (Bio-Rad). Heme staining was performed as described (64). LC-MS/MS analysis of excised bands was performed by the Proteomics Resource Center, Rockefeller University. Membranes for cytochrome spectra were isolated as described above, except TC buffer (10 mM Tris-HCl [pH 7.4], 16 mM cholate) was used instead of phosphate-buffered saline (PBS) for lysis and resuspension of the membrane pellet (9). Reduced minus oxidized cytochrome spectra were recorded on a UV-Vis spectrophotometer (Uvikon XS/XL) at 24°C using a few grains of solid sodium dithionate as reductant and a few drops of 100 or 200 μM potassium ferricyanide as oxidant (9).

Mouse infections. C57BL/6 mice (Jackson Laboratories) were infected using an Inhalation Exposure System (Glas-Col) to deliver ~100 to 200 bacilli per mouse. CFU were quantified by plating serial dilutions of lung and spleen homogenates from 4 mice per strain per time point on 7H10 agar. Procedures involving mice were reviewed and approved by the Institutional Animal Care and Use Committee of Weill Cornell Medical College.

Whole genome sequencing and analysis. The ΔCcsX strain and a large-colony suppressor mutant were sequenced using an Illumina Genome Analyzer IIx. Approximately 5 μg of DNA was processed using the standard Illumina sample preparation protocol (Illumina, Inc.), and the samples were sequenced in paired-end mode with a read length of 54 bp. The genome was assembled by mapping reads to the parental H37Rv genome and calling single-nucleotide polymorphisms and insertions/deletions as described (65). The mean depths of coverage (number of reads covering each site) were 27.9× and 101.2× for the two strains.

SUPPLEMENTAL MATERIAL

Supplemental material for this article may be found at http://mbio.asm.org/lookup/suppl/doi:10.1128/mBio.00475-13/-/DCSupplemental.

Figure S1, TIF file, 0.9 MB.
Figure S2, TIF file, 1.3 MB.
Figure S3, TIF file, 0.3 MB.
Figure S4, TIF file, 0.4 MB.
Figure S5, TIF file, 1.4 MB.

ACKNOWLEDGMENTS

We thank Nick E. Le Brun for technical advice regarding heme staining and Dirk Schnappinger for critical reading of the manuscript.

This work was partially supported by National Institutes of Health award AI081725. J.L.S. was supported by National Institutes of Health Medical Scientist Training Program grant T32GM07739 to the Weill Cornell/Rockefeller/Sloan-Kettering Tri-Institutional MD-PhD Program.

REFERENCES

1. **Lin PL, Rodgers M, Smith L, Bigbee M, Myers A, Bigbee C, Chiosea I, Capuano SV, Fuhrman C, Klein E, Flynn JL.** 2009. Quantitative comparison of active and latent tuberculosis in the cynomolgus macaque model. Infect. Immun. **77:**4631–4642.
2. **Barry CE, Boshoff HI, Dartois V, Dick T, Ehrt S, Flynn J, Schnappinger D, Wilkinson RJ, Young D.** 2009. The spectrum of latent tuberculosis: rethinking the biology and intervention strategies. Nat. Rev. Microbiol. **7:**845–855.
3. **Kaplan G, Post FA, Moreira AL, Wainwright H, Kreiswirth BN, Tanverdi M, Mathema B, Ramaswamy SV, Walther G, Steyn LM, Barry CE, Bekker LG.** 2003. *Mycobacterium tuberculosis* growth at the cavity surface: a microenvironment with failed immunity. Infect. Immun. **71:**7099–7108.
4. **Ryan GJ, Hoff DR, Driver ER, Voskuil MI, Gonzalez-Juarrero M, Basaraba RJ, Crick DC, Spencer JS, Lenaerts AJ.** 2010. Multiple *M. tuberculosis* phenotypes in mouse and guinea pig lung tissue revealed by a dual-staining approach. PLoS One **5:**e11108. doi: 10.1371/journal.pone.0011108.
5. **Haapanen JH, Kass I, Gensini G, Middlebrook G.** 1959. Studies on the gaseous content of tuberculous cavities. Am. Rev. Respir. Dis. **80:**1–5.
6. **Via LE, Lin PL, Ray SM, Carrillo J, Allen SS, Eum SY, Taylor K, Klein E, Manjunatha U, Gonzales J, Lee EG, Park SK, Raleigh JA, Cho SN, McMurray DN, Flynn JL, Barry CE.** 2008. Tuberculous granulomas are hypoxic in guinea pigs, rabbits, and nonhuman primates. Infect. Immun. **76:**2333–2340.
7. **Poole RK, Cook GM.** 2000. Redundancy of aerobic respiratory chains in bacteria? Routes, reasons and regulation. Adv. Microb. Physiol. **43:**165–224.
8. **Kana B, Machowski E, Schechter N, Teh J, Rubin H, Mizrahi V.** 2009. Electron transport and respiration in mycobacteria, p 35–64. *In* Parish T, Brown A (ed), Mycobacterium: genomics molecular biology, vol **3**. Caister Academic Press, Poole, United Kingdom.
9. **Kana BD, Weinstein EA, Avarbock D, Dawes SS, Rubin H, Mizrahi V.** 2001. Characterization of the cydAB-encoded cytochrome *bd* oxidase from *Mycobacterium smegmatis*. J. Bacteriol. **183:**7076–7086.
10. **Boshoff HI, Barry CE.** 2005. Tuberculosis—metabolism and respiration in the absence of growth. Nat. Rev. Microbiol. **3:**70–80.
11. **Weinstein E, Duncan K, Rubin H.** 2005. Inhibitors of type II NADH: menaquinone oxidoreductase represent a class of antitubercular drugs. Proc. Natl. Acad. Sci, U. S. A. **22:**4548–4553.
12. **Matsoso LG, Kana BD, Crellin PK, Lea-Smith DJ, Pelosi A, Powell D, Dawes SS, Rubin H, Coppel RL, Mizrahi V.** 2005. Function of the cytochrome bc_1-aa_3 branch of the respiratory network in mycobacteria and network adaptation occurring in response to its disruption. J. Bacteriol. **187:**6300–6308.
13. **Thöny Meyer L.** 1997. Biogenesis of respiratory cytochromes in bacteria. Microbiol. Mol. Biol. Rev. **61:**337–376.
14. **Kranz RG, Beckett CS, Goldman BS.** 2002. Genomic analyses of bacterial respiratory and cytochrome *c* assembly systems: *Bordetella* as a model for the system II cytochrome *c* biogenesis pathway. Res. Microbiol. **153:**1–6.
15. **Page MD, Ferguson SJ.** 1990. Apo forms of cytochrome c550 and cytochrome CD1 are translocated to the periplasm of *Paracoccus denitrificans* in the absence of haem incorporation caused either mutation or inhibition of haem synthesis. Mol. Microbiol. **4:**1181–1192.
16. **Cole ST, Brosch R, Parkhill J, Garnier T, Churcher C, Harris D, Gordon**

SV, Eiglmeier K, Gas S, Barry CE, Tekaia F, Badcock K, Basham D, Brown D, Chillingworth T, Connor R, Davies R, Devlin K, Feltwell T, Gentles S, Hamlin N, Holroyd S, Hornsby T, Jagels K, Krogh A, McLean J, Moule S, Murphy L, Oliver K, Osborne J, Quail MA, Rajandream MA, Rogers J, Rutter S, Seeger K, Skelton J, Squares R, Squares S, Sulston JE, Taylor K, Whitehead S, Barrell BG. 1998. Deciphering the biology of *Mycobacterium tuberculosis* from the complete genome sequence. Nature **393:**537–544.

17. **Goldman BS, Beck DL, Monika EM, Kranz RG.** 1998. Transmembrane heme delivery systems. Proc. Natl. Acad. Sci. U. S. A. **95:**5003–5008.
18. **Le Brun NE, Bengtsson J, Hederstedt L.** 2000. Genes required for cytochrome *c* synthesis in *Bacillus subtilis*. Mol. Microbiol. **36:**638–650.
19. **Beckett CS, Loughman JA, Karberg KA, Donato GM, Goldman WE, Kranz RG.** 2000. Four genes are required for the system II cytochrome *c* biogenesis pathway in Bordetella pertussis, a unique bacterial model. Mol. Microbiol. **38:**465–481.
20. **Ahuja U, Kjelgaard P, Schulz BL, Thöny Meyer L, Hederstedt L.** 2009. Haem-delivery proteins in cytochrome *c* maturation system II. Mol. Microbiol. **73:**1058–1071.
21. **Kranz RG, Richard-Fogal C, Taylor JS, Frawley ER.** 2009. Cytochrome *c* biogenesis: mechanisms for covalent modifications and trafficking of heme and for heme-iron redox control. Microbiol. Mol. Biol. Rev. **73:**510–528.
22. **Lew JM, Kapopoulou A, Jones LM, Cole ST.** 2011. TubercuList—10 years after. Tuberculosis **91:**1–7.
23. **Sonnhammer EL, von Heijne G, Krogh A.** 1998. A hidden Markov model for predicting transmembrane helices in protein sequences. Proc. Int. Conf. Intell. Syst. Mol. Biol. **6:**175–182.
24. **Manoil C, Beckwith J.** 1986. A genetic approach to analyzing membrane protein topology. Science **233:**1403–1408.
25. **Braunstein M, Griffin TJ, Kriakov JI, Friedman ST, Grindley ND, Jacobs WR.** 2000. Identification of genes encoding exported *Mycobacterium tuberculosis* proteins using a Tn552'phoA in vitro transposition system. J. Bacteriol. **182:**2732–2740.
26. **Bertrand T, Eady NA, Jones JN, Jesmin Nagy JM, Jamart-Grégoire B, Raven EL, Brown KA.** 2004. Crystal structure of *Mycobacterium tuberculosis* catalase-peroxidase. J. Biol. Chem. **279:**38991–38999.
27. **Pinto R, Harrison JS, Hsu T, Jacobs WR, Jr, Leyh TS.** 2007. Sulfite reduction in mycobacteria. J. Bacteriol. **189:**6714–6722.
28. **Schnell R, Sandalova T, Hellman U, Lindqvist Y, Schneider G.** 2005. Siroheme- and [Fe4-S4]-dependent NirA from *Mycobacterium tuberculosis* is a sulfite reductase with a covalent Cys-Tyr bond in the active site. J. Biol. Chem. **280:**27319–27328.
29. **Bali S, Lawrence AD, Lobo SA, Saraiva LM, Golding BT, Palmer DJ, Howard MJ, Ferguson SJ, Warren MJ.** 2011. Molecular hijacking of siroheme for the synthesis of heme and d_1 heme. Proc. Natl. Acad. Sci. U. S. A. **108:**18260–18265.
30. **de Souza GA, Leversen NA, Målen H, Wiker HG.** 2011. Bacterial proteins with cleaved or uncleaved signal peptides of the general secretory pathway. J. Proteomics. **75:**502–510.
31. **Målen H, Pathak S, Søfteland T, de Souza GA, Wiker HG.** 2010. Definition of novel cell envelope associated proteins in Triton X-114 extracts of *Mycobacterium tuberculosis* H37Rv. BMC Microbiol. **10:**132.
32. **Jones CW, Poole RK.** 1985. The analysis of cytochromes, p 285–328. In Gottschalk G (ed), Methods in microbiology, vol **18**. Academic Press, London, United Kingdom.
33. **Boshoff HI, Myers TG, Copp BR, McNeil MR, Wilson MA, Barry CE.** 2004. The transcriptional responses of *Mycobacterium tuberculosis* to inhibitors of metabolism. J. Biol. Chem. **279:**40174–40184.
34. **Yano T, Li LS, Weinstein E, Teh JS, Rubin H.** 2006. Steady-state kinetics and inhibitory action of antitubercular phenothiazines on *Mycobacterium tuberculosis* type-II NADH-menaquinone oxidoreductase (NDH-2). J. Biol. Chem. **281:**11456–11463.
35. **Sassetti CM, Boyd DH, Rubin EJ.** 2001. Comprehensive identification of conditionally essential genes in mycobacteria. Proc. Natl. Acad. Sci. U. S. A. **98:**12712–12717.
36. **Griffin JE, Gawronski JD, Dejesus MA, Ioerger TR, Akerley BJ, Sassetti CM.** 2011. High-resolution phenotypic profiling defines genes essential for mycobacterial growth and cholesterol catabolism. PLoS Pathog. **7:**e1002251. doi:10.1371/journal.ppat.1002251.
37. **Tanboon W, Chuchue T, Vattanaviboon P, Mongkolsuk S.** 2009. Inactivation of thioredoxin-like gene alters oxidative stress resistance and reduces cytochrome *c* oxidase activity in *Agrobacterium tumefaciens*. FEMS Microbiol. Lett. **295:**110–116.
38. **Achard ME, Hamilton AJ, Dankowski T, Heras B, Schembri MS, Edwards JL, Jennings MP, McEwan AG.** 2009. A periplasmic thioredoxin-like protein plays a role in defense against oxidative stress in *Neisseria gonorrhoeae*. Infect. Immun. **77:**4934–4939.
39. **Sherman DR, Sabo PJ, Hickey MJ, Arain TM, Mahairas GG, Yuan Y, Barry CE, Stover CK.** 1995. Disparate responses to oxidative stress in saprophytic and pathogenic mycobacteria. Proc. Natl. Acad. Sci. U. S. A. **92:**6625–6629.
40. **Jaeger T, Budde H, Flohé L, Menge U, Singh M, Trujillo M, Radi R.** 2004. Multiple thioredoxin-mediated routes to detoxify hydroperoxides in *Mycobacterium tuberculosis*. Arch. Biochem. Biophys. **423:**182–191.
41. **Ng VH, Cox JS, Sousa AO, MacMicking JD, McKinney JD.** 2004. Role of KatG catalase-peroxidase in mycobacterial pathogenesis: countering the phagocyte oxidative burst. Mol. Microbiol. **52:**1291–1302.
42. **Voskuil MI, Bartek IL, Visconti K, Schoolnik GK.** 2011. The response of mycobacterium tuberculosis to reactive oxygen and nitrogen species. Front. Microbiol. **2:**1–12.
43. **Bryk R, Lima CD, Erdjument-Bromage H, Tempst P, Nathan C.** 2002. Metabolic enzymes of mycobacteria linked to antioxidant defense by a thioredoxin-like protein. Science **295:**1073–1077.
44. **Springer B, Master S, Sander P, Zahrt T, McFalone M, Song J, Papavinasasundaram KG, Colston MJ, Boettger E, Deretic V.** 2001. Silencing of oxidative stress response in *Mycobacterium tuberculosis*: expression patterns of *ahpC* in virulent and avirulent strains and effect of *ahpC* inactivation. Infect. Immun. **69:**5967–5973.
45. **Wall D, Delaney JM, Fayet O, Lipinska B, Yamamoto T, Georgopoulos C.** 1992. Arc-dependent thermal regulation and extragenic suppression of the *Escherichia coli* cytochrome *d* operon. J. Bacteriol. **174:**6554–6562.
46. **Lindqvist A, Membrillo-Hernández J, Poole RK, Cook GM.** 2000. Roles of respiratory oxidases in protecting. Escherichia coli K-12 from oxidative stress. Antonie van Leeuwenhoek **78:**23–31.
47. **Kita K, Konishi K, Anraku Y.** 1984. Terminal oxidases of *Escherichia coli* aerobic respiratory chain. II. Purification and properties of cytochrome b_{558}-*d* complex from cells grown with limited oxygen and evidence of branched electron-carrying systems. J. Biol. Chem. **259:**3375–3381.
48. **Kelly MJ, Poole RK, Yates MG, Kennedy C.** 1990. Cloning and mutagenesis of genes encoding the cytochrome *bd* terminal oxidase complex in *Azotobacter vinelandii*: mutants deficient in the cytochrome *d* complex are unable to fix nitrogen in air. J. Bacteriol. **172:**6010–6019.
49. **Paulus A, Rossius SG, Dijk M, de Vries S.** 2012. Oxoferryl-porphyrin radical catalytic intermediate in cytochrome *bd* oxidases protects cells from formation of reactive oxygen species. J. Biol. Chem. **287:**8830–8838.
50. **Shi L, Sohaskey CD, Kana BD, Dawes S, North RJ, Mizrahi V, Gennaro ML.** 2005. Changes in energy metabolism of *Mycobacterium tuberculosis* in mouse lung and under *in vitro* conditions affecting aerobic respiration. Proc. Natl. Acad. Sci. U. S. A. **102:**15629–15634.
51. **Dutton RJ, Boyd D, Berkmen M, Beckwith J.** 2008. Bacterial species exhibit diversity in their mechanisms and capacity for protein disulfide bond formation. Proc. Natl. Acad. Sci. U. S. A. **105:**11933–11938.
52. **Dutton RJ, Wayman A, Wei JR, Rubin EJ, Beckwith J, Boyd D.** 2010. Inhibition of bacterial disulfide bond formation by the anticoagulant warfarin. Proc. Natl. Acad. Sci. U. S. A. **107:**297–301.
53. **Kadokura H, Katzen F, Beckwith J.** 2003. Protein disulfide bond formation in prokaryotes. Annu. Rev. Biochem. **72:**111–135.
54. **Martin JL.** 1995. Thioredoxin—a fold for all reasons. Structure **3:**245–250.
55. **Kadokura H, Tian H, Zander T, Bardwell JC, Beckwith J.** 2004. Snapshots of DsbA in action: detection of proteins in the process of oxidative folding. Science **303:**534–537.
56. **Akiyama Y, Ito K.** 1993. Folding and assembly of bacterial alkaline phosphatase in vitro and in vivo. J. Biol. Chem. **268:**8146–8150.
57. **Deshmukh M, Turkarslan S, Astor D, Valkova-Valchanova M, Daldal F.** 2003. The dithiol:disulfide oxidoreductases DsbA and DsbB of *Rhodobacter capsulatus* are not directly involved in cytochrome *c* biogenesis, but their inactivation restores the cytochrome *c* biogenesis defect of CcdA-null mutants. J. Bacteriol. **185:**3361–3372.
58. **Erlendsson LS, Hederstedt L.** 2002. Mutations in the thiol-disulfide oxidoreductases BdbC and BdbD can suppress cytochrome *c* deficiency of CcdA-defective *Bacillus subtilis* cells. J. Bacteriol. **184:**1423–1429.
59. **Erlendsson LS, Acheson RM, Hederstedt L, Le Brun NE.** 2003. *Bacillus*

subtilis ResA is a thiol-disulfide oxidoreductase involved in cytochrome *c* synthesis. J. Biol. Chem. **278:**17852–17858.
60. **Blumenthal A, Trujillo C, Ehrt S, Schnappinger D.** 2010. Simultaneous analysis of multiple *Mycobacterium tuberculosis* knockdown mutants in vitro and in vivo. PLoS One **5:**e15667. doi: 10.1371/journal.pone.0015667.
61. **Pelicic V, Jackson M, Reyrat JM, Jacobs WR, Gicquel B, Guilhot C.** 1997. Efficient allelic exchange and transposon mutagenesis in *Mycobacterium tuberculosis*. Proc. Natl. Acad. Sci. U. S. A. **94:**10955–10960.
62. **Small JL, O'Donoghue AJ, Boritsch EC, Tsodikov OV, Knudsen GM, Vandal O, Craik CS, Ehrt S.** 2013. Substrate specificity of MarP, a periplasmic protease required for resistance to acid and oxidative stress in *Mycobacterium tuberculosis*. J. Biol. Chem. **288:**12489–12499.
63. **Vandal OH, Pierini LM, Schnappinger D, Nathan CF, Ehrt S.** 2008. A membrane protein preserves intrabacterial pH in intraphagosomal *Mycobacterium tuberculosis*. Nat. Med. **14:**849–854.
64. **Hodson CT, Lewin A, Hederstedt L, Le Brun NE.** 2008. The active-site cysteinyls and hydrophobic cavity residues of ResA are important for cytochrome *c* maturation in *Bacillus subtilis*. J. Bacteriol. **190:**4697–4705.
65. **Ioerger TR, Feng Y, Ganesula K, Chen X, Dobos KM, Fortune S, Jacobs WR, Mizrahi V, Parish T, Rubin E, Sassetti C, Sacchettini JC.** 2010. Variation among genome sequences of H37Rv strains of *Mycobacterium tuberculosis* from multiple laboratories. J. Bacteriol. **192:**3645–3653.
66. **Ehrt S, Schnappinger D.** 2006. Controlling gene expression in mycobacteria. Future Microbiol. **1:**177–184.